

Recent advances in AMS of ^{36}Cl with a 3-MV-tandem

Martin Martschini¹, Oliver Forstner¹, Robin Golser¹, Walter Kutschera¹,
Stefan Pavetich¹, Martin Suter², Alfred Priller¹, Peter Steier¹, Anton Wallner¹



¹ VERA Laboratory, Fakultät für Physik - Isotopenforschung,
Universität Wien, Währinger Straße 17, A-1090 Wien, Austria
² Ion Beam Physics, Department of Physics, ETH Zürich,
Schafmattstraße 20, CH-8093 Zürich, Switzerland



Introduction

Accelerator mass spectrometry (AMS) of ^{36}Cl ($t_{1/2} = 0.30$ Ma) at natural isotopic concentrations requires high particle energies for the separation from the stable isobar ^{36}S and so far was exclusively the domain of tandem-accelerator machines with at least 5 MV terminal voltage. At VERA (Vienna Environmental Research Accelerator) we have performed the first ^{36}Cl exposure dating measurement with a 3 MV tandem accelerator, operating our machine at 3.5 MV, using terminal foil stripping and a split-anode ionization chamber [1]. In a different work, we evaluated the performance of various detectors for ^{36}Cl in order to achieve similar ^{36}S suppression already at lower terminal voltage [2]. While these measurements were done with an exploratory detector setup, considerable effort was necessary to allow routine measurements of ^{36}Cl . These advances are shown below and include investigations of the detection system regarding energy loss and energy straggling in various detector gases and the behavior of the ion source.

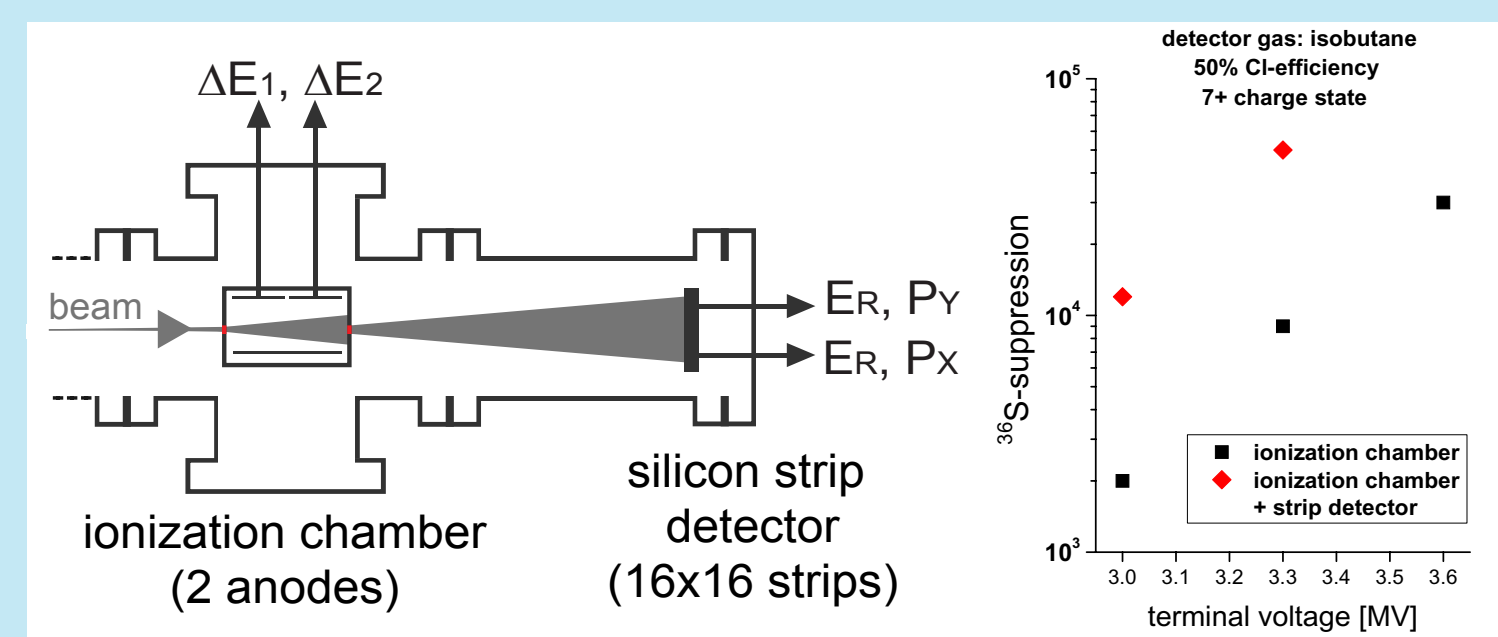


Fig. 2: Schematic of our current detection system for ^{36}Cl providing two independent energy loss measurements ($\Delta E_1, \Delta E_2$), two residual energy measurements (E_{x1}, E_{x2}) and x/y position information (P_x, P_y). The ^{36}S suppression factors strongly depend on the particle energy thus on the terminal voltage.

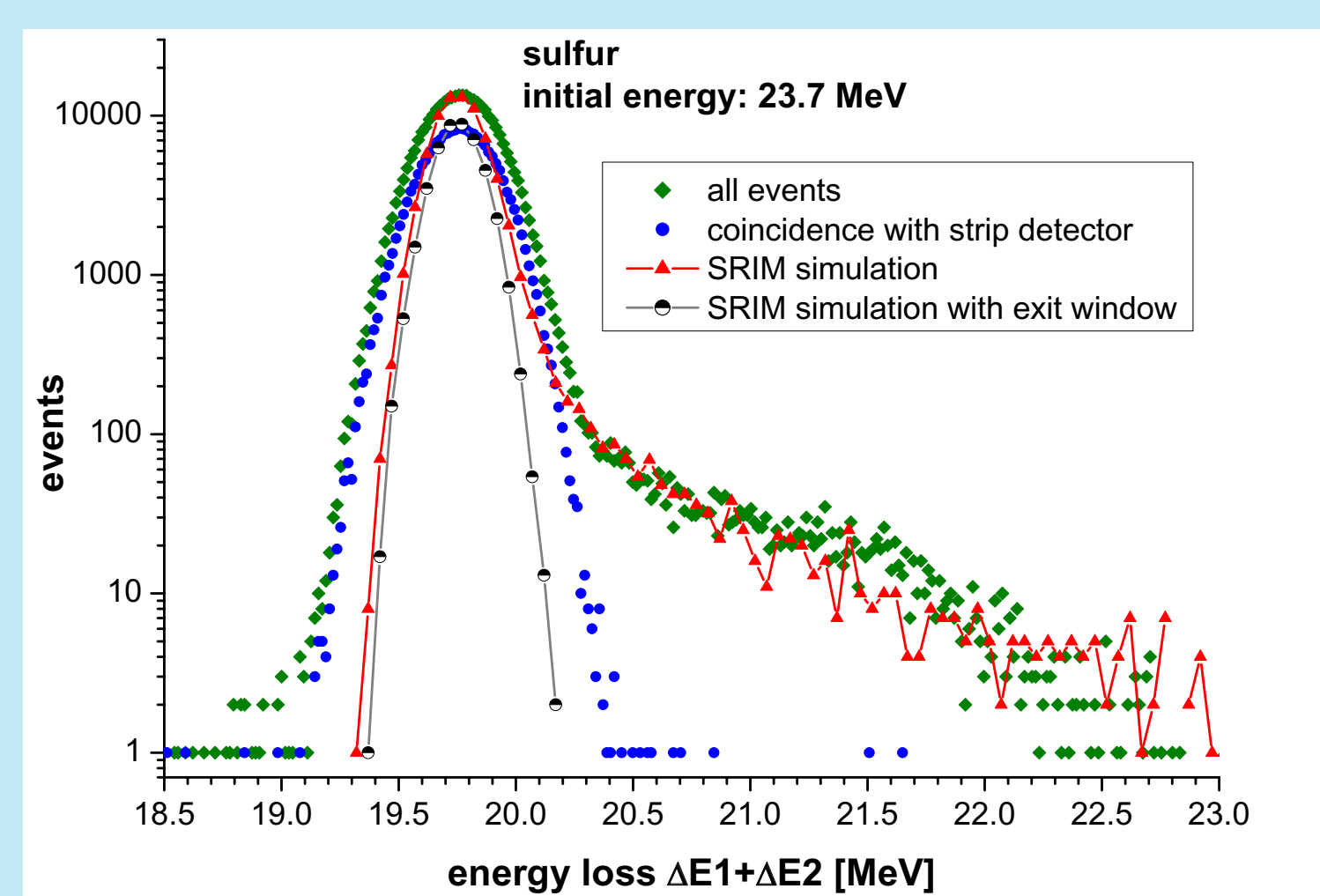


Fig. 3: Comparison of experimental total energy loss spectra from the ionization chamber with a SRIM simulation. Note that the energy tails, which are caused by scattering events (nuclear stopping) are well reproduced in the SRIM simulation, whereas the inner part of the peak, which can be well described with a normal distribution, is predominantly caused by straggling of the electronic stopping process, which is underestimated in the simulation. The initial energy of 23.7 MeV instead of 24.07 MeV compensates for the energy loss in the entrance window.

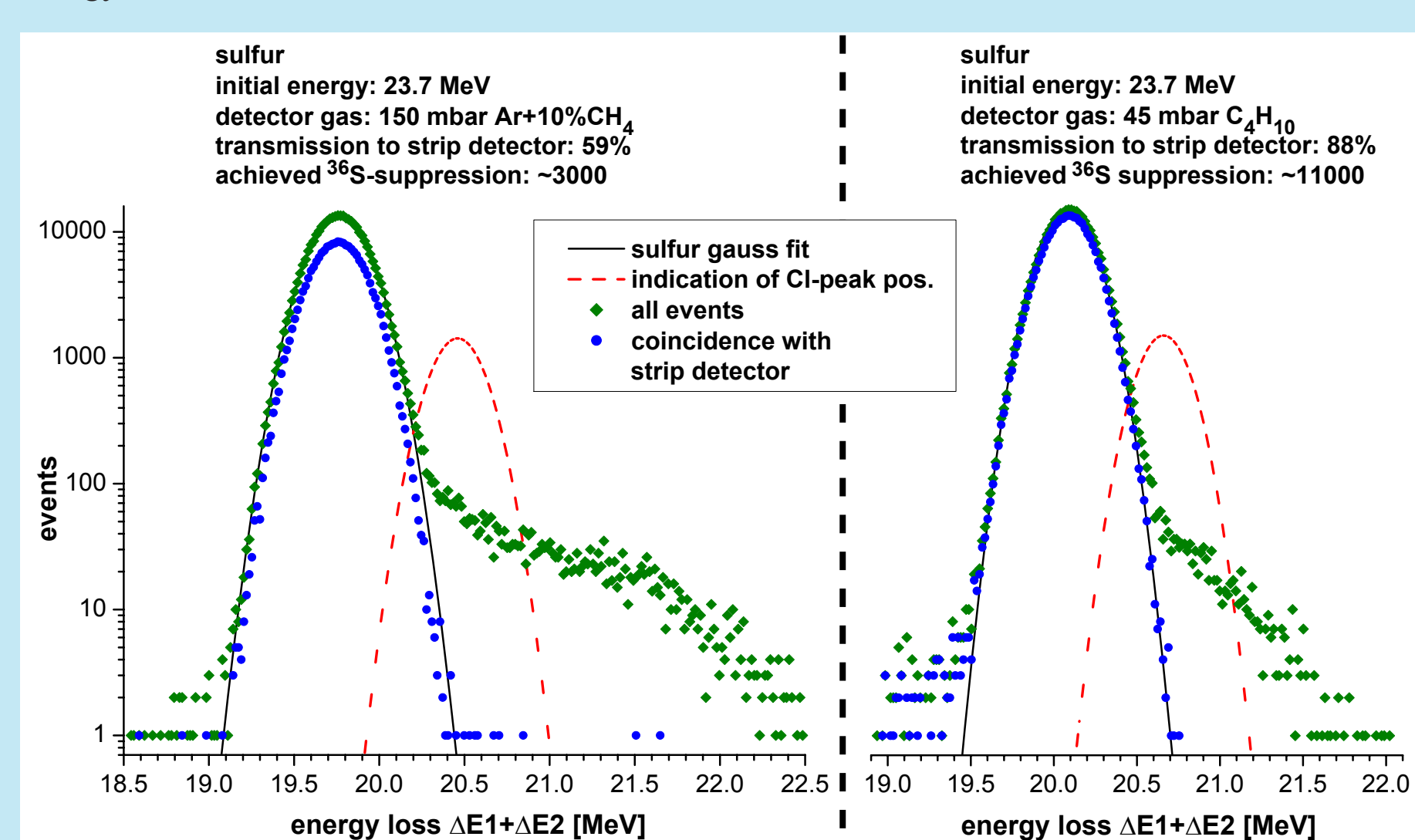


Fig. 4: Comparison of sulfur energy loss spectra recorded on a steel target with the ionization chamber filled with isobutane and argon-methane respectively. The Cl-peak position was determined in different runs on a standard material with $^{36}\text{Cl}/\text{Cl} = 10^{-11}$. Despite better peak separation, Ar+CH₄ does not provide higher ^{36}S suppression because of the pronounced angular scattering tail.

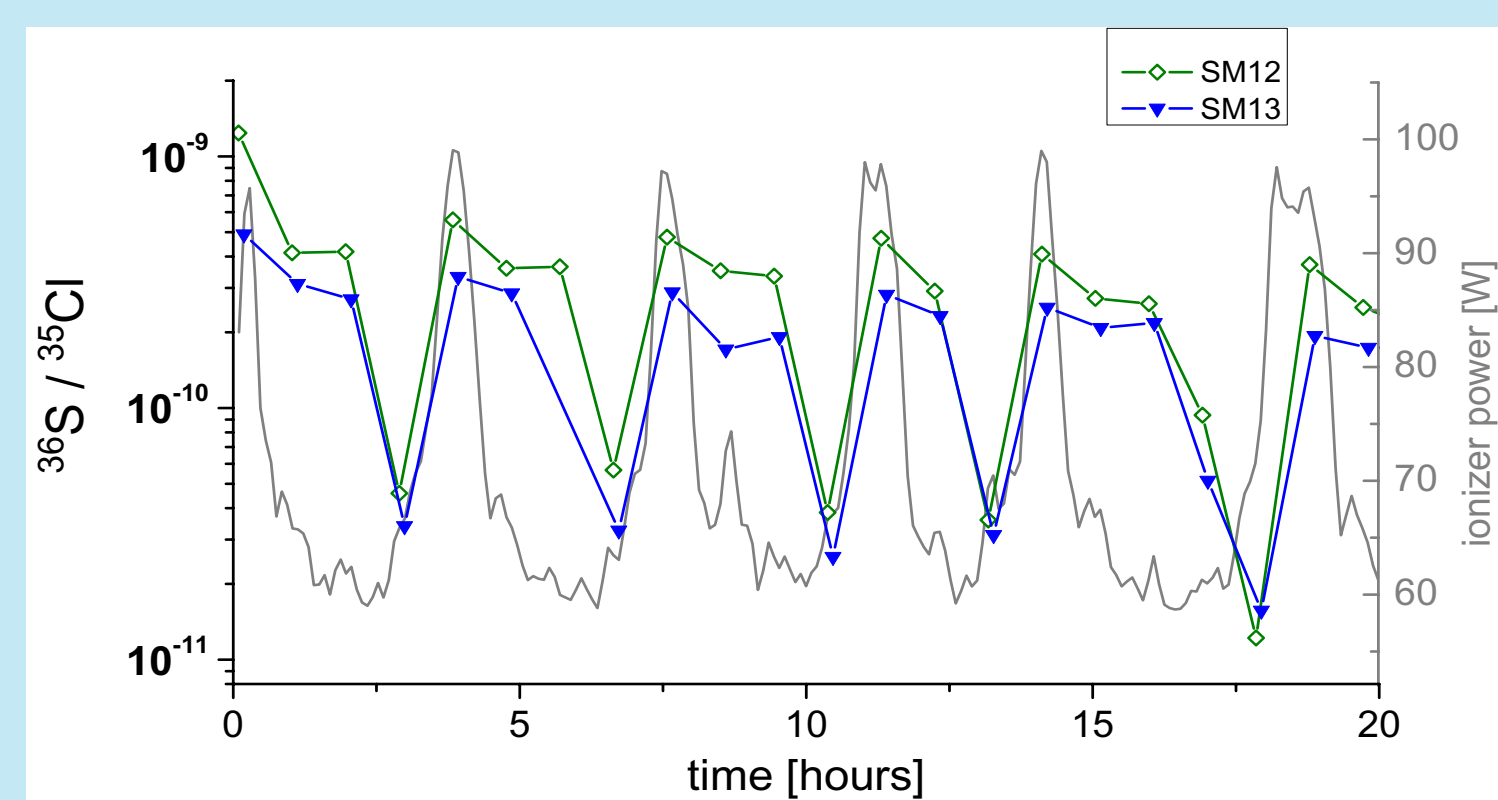


Fig. 6: Sulfur output from two samples (SM12 and SM13) and ionizer power during a 40 hour beam time. Each point shows the results from one run lasting ~5 min. The ionizer power was adjusted to keep the $^{35}\text{Cl}^-$ current almost stable at 1 μA . The regulation was configured badly and oscillating, which revealed a strong dependence of the sulfur output on the ionizer power.

Sample at the beginning of the cycle	First blank in cycle (3 min after standard) $^{36}\text{Cl}/\text{Cl}$	Last blank in cycle (2 h after standard) $^{36}\text{Cl}/\text{Cl}$
initial blank value no standards sputtered yet	$(4 \pm 8) \times 10^{-16}$	$(4 \pm 8) \times 10^{-16}$
10^{-12} sample (standard) sputtered for 5 min	$(2.5 \pm 1.3) \times 10^{-15}$	$(5 \pm 10) \times 10^{-16}$
10^{-11} sample (standard) sputtered for 5 min	$(1.4 \pm 0.2) \times 10^{-14}$	$(3 \pm 1) \times 10^{-15}$
final blank value no standards sputtered for 24h	$(3.0 \pm 0.7) \times 10^{-15}$	$(1.5 \pm 0.5) \times 10^{-15}$

Table 1: The memory effect of the ion source was studied by periodic measurements on a set of blank samples. The table shows the normalized $^{36}\text{Cl}/\text{Cl}$ values after sulfur induced background correction. Independent from the cathode positions, the first blank in the cycle (sputtered right after the standards) also showed the highest final blank value. In our understanding, Cl vapor from the samples also takes part in the sputtering process and therefore is implanted in the following target materials at a level of $\sim 10^{-4}$.

References:

- [1] P. Steier et al., Nucl. Instr. and Meth. in Phys. Res. B **268** (2010) 744-747.
- [2] T. Orłowski et al., Nucl. Instr. and Meth. in Phys. Res. B **268** (2010) 847-850.
- [3] M. Stocker et al., Nucl. Instr. and Meth. in Phys. Res. B **240** (2005) 483-489.
- [4] H. Schmidt-Böcking, H. Hornung, Z. Physik **A286** (1978) 253-261
- [5] M. Suter et al., Nucl. Instr. and Meth. in Phys. Res. B **259** (2007) 165-172

Detector setup and ^{36}S suppression

Our detector setup consists of a split-anode ionization chamber based on a design developed at the ETH Zurich [3], with 5×5 mm silicon nitride entrance and exit windows (100 nm thickness from Silson Ltd, UK) followed by a double-sided silicon strip detector (Micron Semiconductors Design W1, 50×50 mm active area, 256 pixels) sitting 30 cm behind the exit window of the ionization chamber. The best separation is achieved by adjusting the detector gas pressure such, that the ions have lost $\sim 5/6$ of their initial energy when leaving the ionization chamber. The actual ^{36}S suppression depends strongly on the acceptance of the ^{36}Cl gates and thus on the ^{36}Cl detection efficiency. All our ^{36}S suppression values are for 50% ^{36}Cl detection efficiency, including losses caused by angular straggling in the detector system. The ^{36}S suppression factors are determined using an attenuated beam from a stainless steel sample (blank) as the ratio of events in the $^{36}\text{S}^{7+}$ peak versus the number of events in the $^{36}\text{Cl}^{7+}$ integration bin, multiplied by the ^{36}Cl acceptance of the detection system (0.5).

With an additional residual energy signal from the silicon strip detector, ^{36}S suppression factors above 10,000 at 3 MV (24 MeV particle energy) were obtained. This considerable increase is mainly due to the fact that unwanted high energy tails in the ionization chamber spectra arising from angular scattering are suppressed by accepting only events in coincidence with the strip detector. The resulting spectra are Gaussian shaped peaks over several orders of magnitude (Figure 3). As scattered ions have a longer flight path through the chamber and subsequently deposit more of their kinetic energy and also the recoil particles lead to additional ionization, some scattered ^{36}S ions would end up in the ^{36}Cl bin. However, ions with inclined flight paths usually do not pass the exit window aperture of the ionization chamber and are rejected.

^{36}S suppression in various detector gases

Motivated by a work from Schmidt-Böcking [4], we studied three detector gases (argon-methane, isobutane, isobutane-argon) with respect to the parameters determining the ^{36}S suppression: energy loss straggling (peak width), separation between Cl and S peaks and transmission through the detector (angular scattering):

- Argon-methane as detector gas produces $\sim 10\%$ less energy straggling than isobutane over a large range of energy detector loss and at even higher peak separation, although our data suggest a more pronounced energy focusing effect [5] in C_4H_{10} (Figure 5).
- Due to the lower stopping power of Ar-CH₄, a higher gas pressure of 150 mbar had to be used instead of 45 mbar for isobutane. Together with the higher angular scattering cross section of argon, this resulted in a transmission of only 59% through the ionization chamber compared to 90% for isobutane.
- Since the ^{36}Cl bin size had to be chosen accordingly for 50% Cl detection efficiency, we achieved a ^{36}S suppression of only $\sim 3,000$ for Ar-CH₄ and $\sim 11,000$ for C_4H_{10} .
- A mix of the two gases (C_4H_{10} with 30% argon) seems the best compromise between good peak separation and high transmission and yielded a ^{36}S suppression of 20,000.

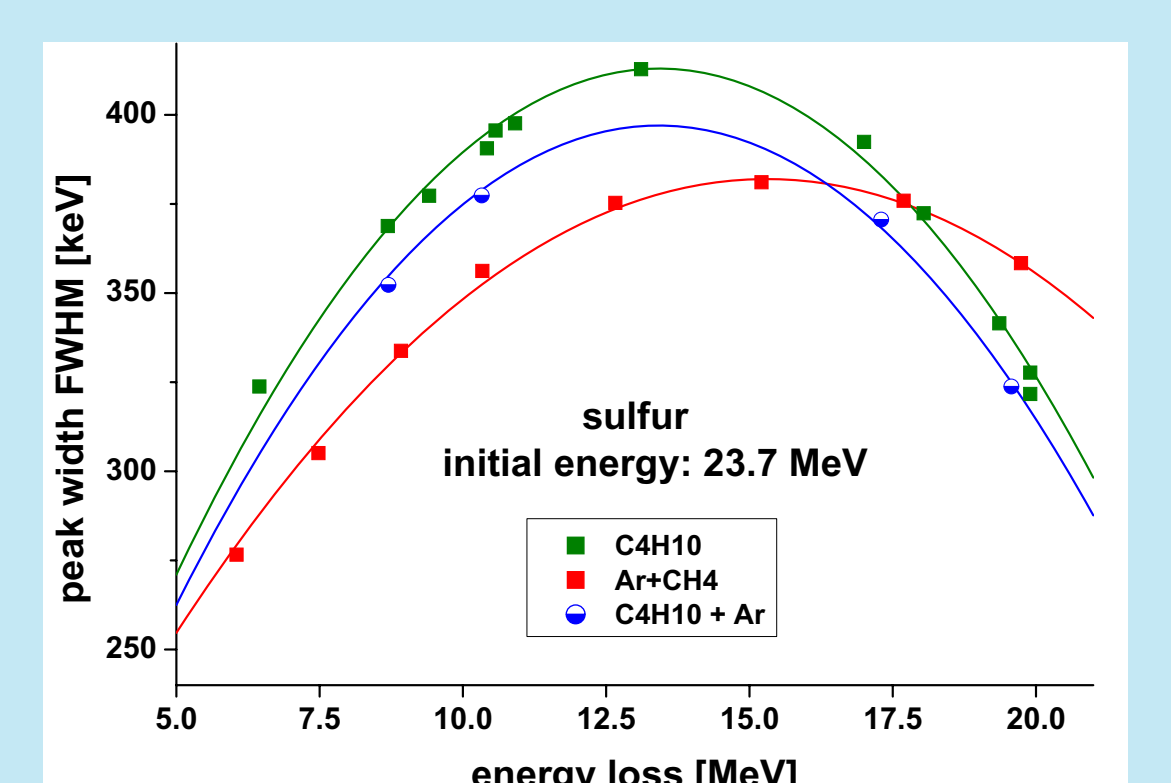


Fig. 5: Energy loss straggling of ^{36}S with an initial energy of 23.7 MeV in various counter gases. The effect of energy focusing [5] occurring below the maximum of the Bragg curve has a strong influence on the peak widths.

Ion source: sulfur and chlorine output, memory effect and cross contamination

We use Cu-cathodes with silver bromide backing (Figure 7) to reduce the sulfur output from our SNICS ion source. We screened different batches of commercially available silver bromide but achieved the best results with our own AgBr produced at the VERA laboratory from KBr cleaned from sulfur by precipitation of BaSO₄. Tantalum plates as backing material and Ni-cathodes (without backing) showed a significantly higher sulfur output than AgBr.

To achieve constant output from our Cs-sputter source, we use the current from the source high voltage power supply for a feedback regulation of the ionizer power, while the cesium oven temperature is kept constant at typical values used for other AMS isotopes. The regulation achieves the same Cl⁻ current on all samples in the wheel typically within 100 s after sample change and keeps it constant within 25%. Our investigations also revealed a strong dependence of the sulfur output on the ionizer power (Figure 6, obtained while the regulation was oscillating). With optimized parameters of the regulation, the average sulfur output from our ion source is $^{36}\text{S}/^{35}\text{Cl}^- \approx 5 \times 10^{-11}$ corresponding to a detector count rate of ~ 300 Hz at 5 μA $^{35}\text{Cl}^-$ -current and a sulfur induced signal in the ^{36}Cl bin of $^{36}\text{Cl}/\text{Cl} \approx 2.5 \times 10^{-15}$.

The influence of memory effect and cross contamination (Table 1) can be mitigated by careful choice of the target order and the use of appropriate standard materials. The blank value of $^{36}\text{Cl}/\text{Cl} = (4 \pm 8) \times 10^{-16}$ is in good agreement with the lowest so far published ratios around 5×10^{-16} and demonstrates that 3 MV tandems can achieve the same sensitivity for ^{36}Cl than larger machines.

Conclusions and Outlook

The reproducibility of the $^{36}\text{Cl}/\text{Cl}$ isotopic ratio measurements is $\sim 2\%$ for 10^{-12} samples. We achieve an injector to detector efficiency for ^{36}Cl ions of 8% (16% stripping yield for the 7+ charge state in the accelerator, 50% ^{36}Cl detection efficiency), which also compares favorably to other facilities. In the near future, we aim to reduce the amount of AgCl required for a decent measurement (currently ~ 4 mg AgCl) and advances have already been made with samples ≤ 1 mg AgCl.

Recently, based on the development described in this paper, more successful measurements on real exposure dating samples in the range of $^{36}\text{Cl}/\text{Cl} = 3 \times 10^{-14}$ to 10^{-11} have been successfully performed (results will be published separately). This further demonstrates that measurements competitive to larger tandems are possible at 3 MV terminal voltage.

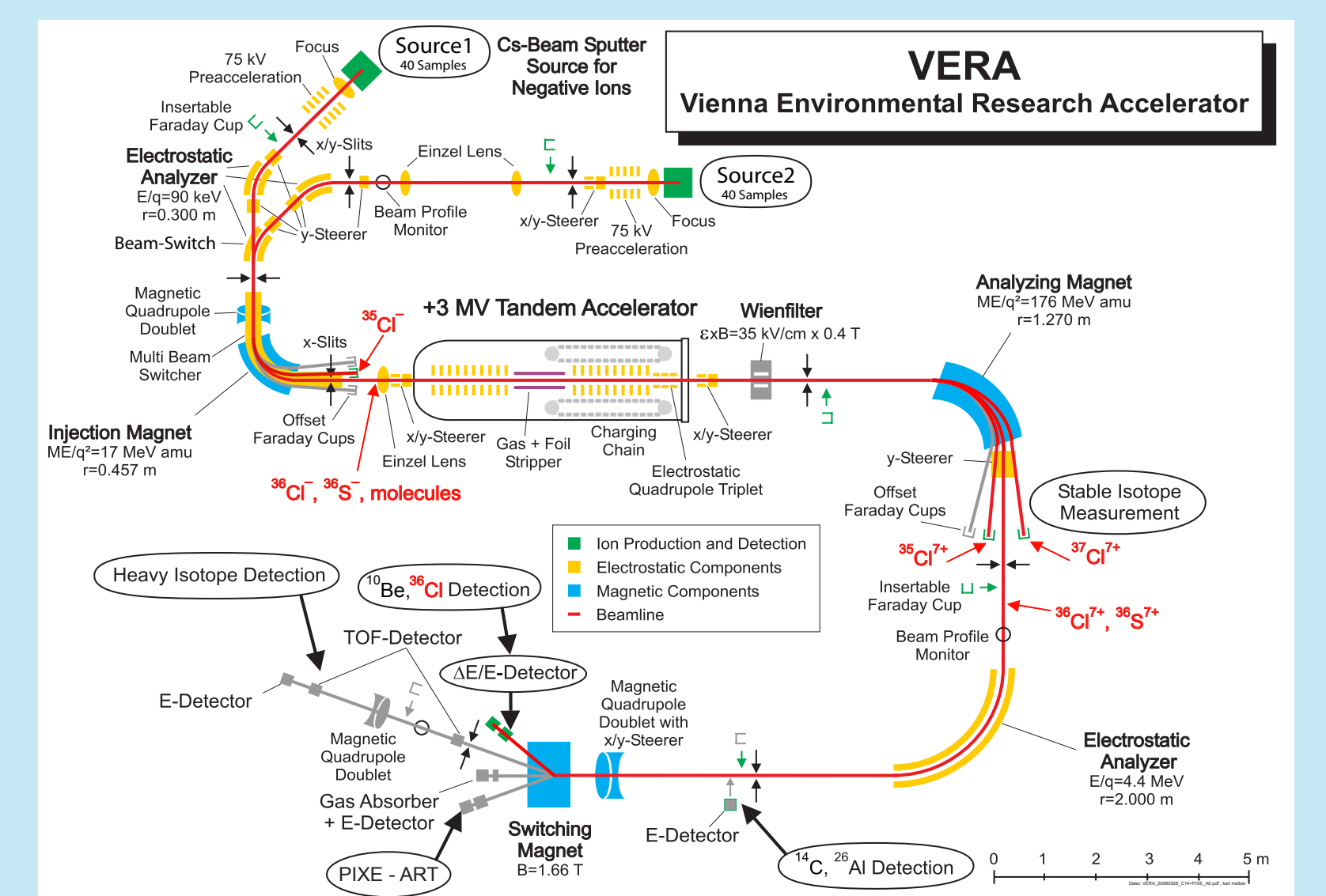


Fig. 1: Setup of VERA for ^{36}Cl measurements in 2010

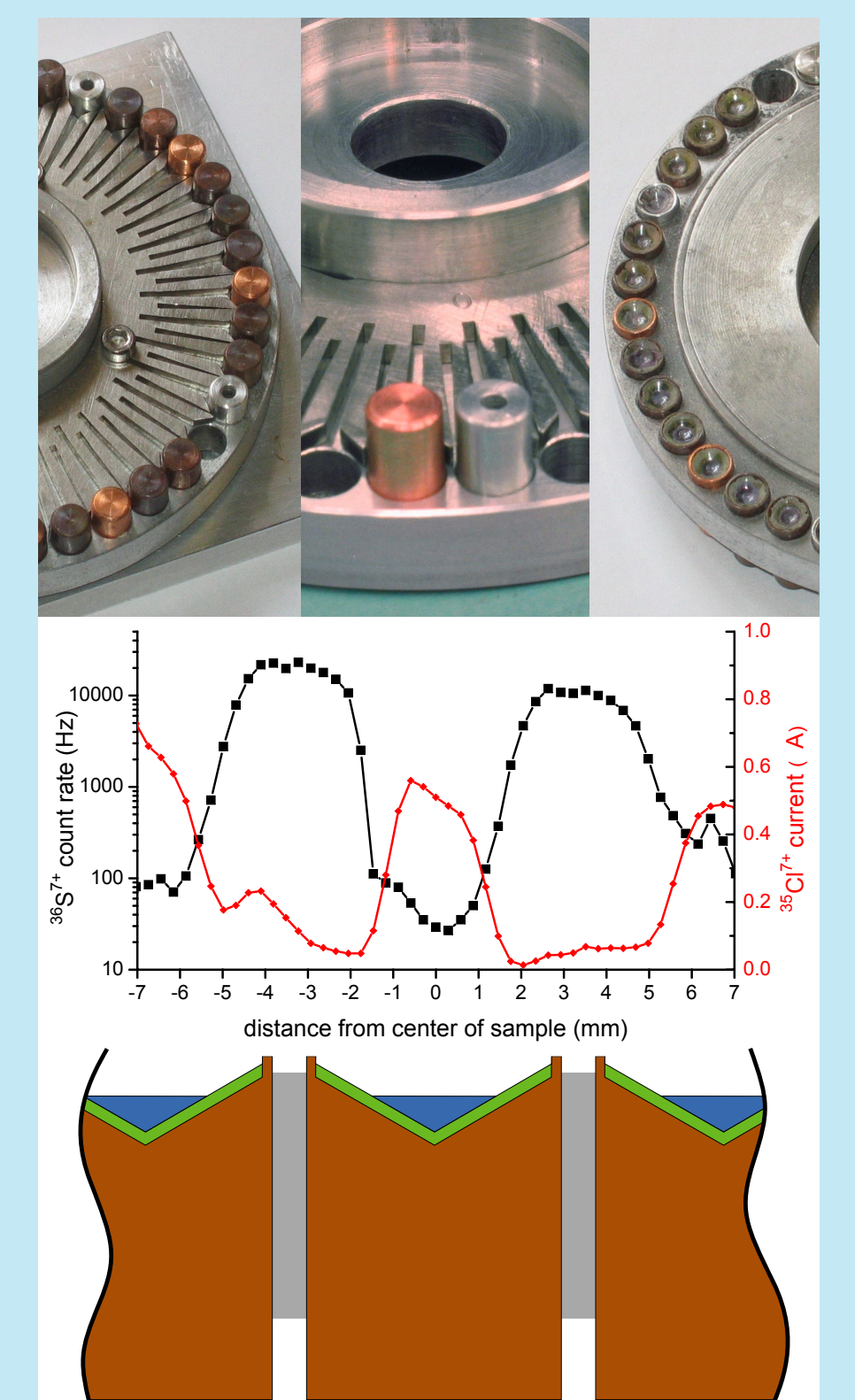


Fig. 7: The photos show the new sample wheel for 40 samples, which are held by clips on the backside of the wheel. The schematic shows a cut through 3 target in the wheel: 6mm Cu-cylinders (brown) with a 5mm conical hole coated with AgBr (green) and the AgCl sputter target (blue) pressed in the center. The plot above the schematic shows the $^{36}\text{S}^{7+}$ count rate and the $^{35}\text{Cl}^{7+}$ current during a scan over the target surface. The x-axis of the plot and the schematic are matched.